Stereocopolyamides Derived from 2,3-Di-*O*-Methyl-D- and -L-Tartaric Acids and Hexamethylenediamine. 2. Influence of the Configurational Composition on the Crystal Structure of Optically Compensated Systems

I. Iribarren, C. Alemán, C. Regaño, A. Martínez de Ilarduya, J. J. Bou, and S. Muñoz-Guerra*

Departament d'Enginyeria Química, Universitat Politécnica de Catalunya ETSEIB, Diagonal, 647, 08028 Barcelona, Spain

Received March 28, 1996; Revised Manuscript Received September 12, 1996[⊗]

ABSTRACT: The crystal structure of both the racemic copolyamide obtained from the racemic mixture of 2,3-di-*O*-methyl-D- and -L-tartaric acids and hexamethylenediamine and the equimolar mixture of the two configurationally homogeneous D- and L-polyamides was investigated with reference to the structure previously described for the optically pure poly(hexamethylene-2,3-di-*O*-methyl-L-tartaramide). DSC measurements showed that the two optically compensated systems have a crystallinity comparable to that displayed by the pure enantiomorphs whereas solid state cross-polarization−magic angle spinning ^{13}C NMR spectra revealed structural differences between optically active and inactive forms. Structural data provided by X-ray diffraction and electron microscopy of powders, fibers, and single crystals were used for establishing the crystal structures of the inactive forms. In these systems the polymer chain assumed the same contracted conformation adopted by the optically pure polymer. The CERIUS[2] software package was used for building the crystal models which were further adjusted on-line by diffraction pattern simulation. The crystal structure of the equimolar mixture of the two optically pure polymers could be satisfactorily represented by a monoclinic unit cell containing two enantiomeric chains related by a glide plane. A similar model appeared to be adequate for the racemic copolyamide if the crystal lattice is assumed to be composed of configurationally averaged identical chains. In both cases, the arrangement of the chains within the crystal turns to be substantially the same as that adopted in the triclinic structure of the optically pure polymer. Energy calculations corroborated the ability of D- and L-tartaric units to cocrystallize without significant distortion of the geometry of the crystal lattice.

Introduction

Polytartaramides, *i.e.* polyamides derived from tartaric acid, have been recently object of a sustained investigation addressed to explore their potential as new biodegradable materials.[1−4] A variety of types of polytartaramides differing either in the diamine used as comonomer or in the nature of the side groups attached to tartaric acid has been synthesized, and their properties have been systematically evaluated in connection with the chemical constitution.[5−8] Among them, polytartaramides obtained from 2,3-di-*O*-methyl-L-tartaric acid and 1,*n*-alkanediamines, which are referred in the literature as P*n*DMLT, have been studied in greater detail since they display desirable average properties and their preparation is relatively easy.

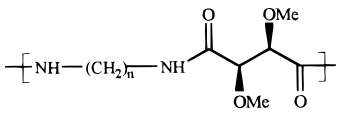

P*n*DMLT

The repeating unit of P*n*DMLT contains two vicinal asymmetric backbone carbons in a *threo* configuration. Since L-tartaric acid has C_2 symmetry, no configurational disorder due to orientation effects may arise into the growing polytartaramide chain during polycondensation. Accordingly, stereoregular polymers with a *threodiisotactic* microstructure will be obtained provided that polymerization conditions preventing racemization reactions are used. In a previous work,[9] we analyzed the crystal structure of P*n*DMLT with particular attention given to poly(hexamethylene-2,3-di-*O*-methyl-L-tartaramide), P6DMLT. It was found there that P*n*DMLT are highly crystalline polymers, which is by no means a property usually found among substituted polyamides. Energy calculations revealed that a *gauche* conformation is the arrangement preferred by the tartaric moiety in these polytartaramides and X-ray diffraction evidenced that they crystallize in a slightly folded conformation, implying a shortening of the repeating unit length by about 2 Å. A triclinic lattice in the space group *P*1 with hydrogen bonds intermolecularly set was proposed to be the crystal structure commonly adopted by the whole series. The dimensions of the unit cell for P6DMLT are $a = 5.00$ Å, $b = 6.84$ Å, $c = 13.20$ Å, $\alpha = 61.5°$, $\beta = 90.0°$, and $\gamma = 111.6°$. Computational modeling showed that the structure may be described as a stack of hydrogen-bonded sheets staggered in a regular manner with features reminiscent of both the β-pleated sheet form of polypeptides and the triclinic α-form of nylon 66.

In part 1 of this work, the influence of the configurational composition on properties of poly(hexamethylene-2,3-di-*O*-methyl-D,L-tartaramide)s, P6DM(D,L)T, was throughout examined.[10] Random stereocopolyamides containing variable amounts of D- and L-tartaric units were synthesized and their properties compared with those displayed by the optically pure polymer.

It was found there that the crystallinity of these polytartaramides is not severely affected by variations in the enantiomeric composition. Furthermore, certain properties closely related to the structure in the solid state appeared to be practically indistinguishable when

* To whom all correspondence should be addressed.
[⊗] Abstract published in *Advance ACS Abstracts,* November 1, 1996.

S0024-9297(96)00473-1 CCC: $12.00

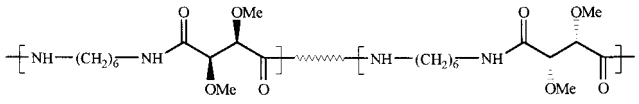

P6DM(D,L)T

the racemic copolyamide P6DM(D,L)T (1:1) and the optically pure polyamide P6DMLT were compared. Preliminary powder X-ray diffraction results were consistent with such findings; the only structural difference between the two polyamides that could be perceived by this technique consisted of a weak reflection at 4.9 Å appearing in the diagrams of the racemic compound.

The fact that poly(hexamethylene-di-*O*-methyl-D,L-tartaramide)s are able to crystallize as if they were optically pure polymers is an interesting finding. Whereas isomorphic replacement is a phenomenon common among low molecular weight compounds, statistical stereocopolymers as well as mixtures of enantiomorphic polymers are leaning to crystallize in separated phases.[11] Such a tendency increases with the number of stereocenters per repeating unit and is even more pronounced in hydrogen-bond-forming polymers, as is indeed the case with the polyamides concerned in this work. Nevertheless, the number of polymeric racemate mixtures reported to be crystalline is incessantly increasing since Dumas *et al*. first described a stereocomplex for poly(*tert*-butylthiirane) which crystallizes in a structure different from that of the corresponding isotactic polymers.[12] At present, a fair number of examples covering a wide variety of constitutions may be found in the literature.[13] In all cases, the repeating unit of the polymer contains only one stereocenter which is usually located in the main chain. Crystallization of the racemate mixture usually results from the stereoselective association that takes place in the liquid state between the corresponding optically active polymers. Detailed studies performed on stereocomplexation both in the melt[14] and in solution[15] have revealed that the stereocomplex entails a molecular interaction more favorable than that that would occur in the case of self-association.

In this paper we study the effect of the stereochemical configuration of the tartaric unit on the crystal structure of polytartaramides deriving from 2,3-di-*O*-methyltartaric acid and hexamethylenediamine. The purpose of the work is to elucidate how the replacement of the L-tartaric unit by its antipode may occur in the crystal without apparent distortion of the lattice. Our approach includes the study of both the random stereocopolyamide P6DM(D,L)T (1:1) and the equimolar mixture of P6DMDT and P6DMLT enantiomorphs, which will be called henceforth P6DM(D,L)T and P6DM(D+L)T, respectively. The crystal structure of these two optically compensated systems is examined by X-ray diffraction, solid state NMR, and electron microscopy and compared with the structure of optically pure P6DMLT. The conclusions to be drawn from this study will be of relevance to the design of novel polyamides made of optically active monomers, in particular of those using carbohydrates derivatives as starting materials.[16]

Experimental Section

Polymer Samples. The synthesis of polytartaramide P6DMLT from L-tartaric acid and hexamethylenediamine by polycondensation applying the active ester method has been reported earlier.[6] In this work, exactly the same procedure has been employed for the preparation of the enantiomorph P6DMDT. In part 1 of this work,[10] the synthesis and characterization of racemic stereocopolyamides consisting either of a random distribution of D- and L-units, [P6DM(D,L)T], or an aregic sequence of (D−L)-units, [P6DM(D−L)T], was described in full detail and their properties compared with those exhibited by the optically pure polymer P6DMLT. A brief account of the most relevant characteristics of the polymers with regard to the present study is given in Table 1.

Table 1. Characteristics of the Polyamides Used in This Work

polyamide	$[\alpha]^{25}_D$ (deg)[a]	$[\eta]$ (dL g^{-1})[b]	M_w[c]	M_n[c]	PD[c]
P6DMDT	−92.5	0.87	22 300	11 400	1.9
P6DMLT	+90.4	0.85	17 100	8 100	2.1
P6DM(D,L)T	+2.00	2.09	50 200	22 500	2.2
P6DM(D-L)T		0.30	5 000	2 900	1.7

[a] Specific optical rotation measured in chloroform. [b] Intrinsic viscosity measured in dichloroacetic acid. [c] Average molecular weights an polydispersities determined by GPC on trifluoroacetylated samples against polystyrene standards.

Experimental Techniques. P6DM(D+L)T samples to be used for X-ray diffraction studies, in both powder and fiber forms, were prepared as follows: Equimolar amounts of the two enantiomers were dissolved in chloroform, and the solution was left stirring for 1 day. The resulting gelly mass was diluted with trifluoroethanol and the mixture was further stirred for another day. The racemate was precipitated from the viscous solution by adding ethyl ether and repeatedly washed with the same solvent. The product was dried to constant weight and stored under vacuum.

Lamellar crystals obtained by crystallization from diluted solutions were mostly used throughout this work. Crystallizations were carried out from solution in polyols at polymer concentrations ≤0.1% w/w under a nitrogen atmosphere. The polymer or polymer mixture was dissolved at a temperature near to 200 °C and then left to crystallize at a fixed temperature for a period of 2−3 h. The resulting suspensions of crystals were quietly filtered, washed repeatedly with 1-butanol and dried under vacuum. The collected sediments were used for X-ray diffraction, differential scanning calorimetry (DSC), and NMR studies. For electron microscopy, drops of the crystal suspensions were removed prior to filtering and deposited on carbon-coated grids.

Density measurements were carried out at 25 °C by the flotation method in mixtures of water and 25% (w/w) KBr aqueous solution. DSC measurements were carried out on a Perkin-Elmer DSC-4 calorimeter under a nitrogen atmosphere. X-ray diffraction diagrams were recorded in a Statton-type camera with nickel-filtered Cu Kα radiation of wavelength of 1.542 Å and were calibrated with molybdenum sulfide (d_{002} = 6.147 Å). Reflection intensities were estimated by a unidimensional Joyce Loebl MK III CS microdensitometer. Electron microscopy was performed on a Phillips EM-301 instrument operating at 80 and 100 kV for bright field and electron diffraction, respectively. For morphological observations, crystals were shadowed with platinum−carbon at an angle of approximately 15°. For electron diffraction, unshadowed crystals were observed at the minimum flux of electrons and diagrams were internally calibrated with gold (d_{111} = 2.35 Å).

Solid state ^{13}C NMR spectra were recorded at 25 °C on a Bruker AMX-300 instrument equipped with a cross-polarization−magic angle spinning (CP−MAS) accessory. A 80−150 mg sample of crystal sediments were spun at 4 kHz in a cylindrical ceramic rotor and spectra acquired with contact and repetition times of 2 ms and 5 s, respectively. A number of transients between 2000 and 12 000 were summed up to build the final spectra. All the spectra were referenced to the higher field peak of adamantane (29.5 ppm).

Energy Calculations and Molecular Modeling. Energy calculations for an isolated polymer chain were performed with the AM1[17] method applied to a suitable model compound containing two successive tartaric units in opposite configuration. Contour maps of the dihedrals involved in the conformation of the tartaric backbone were constructed by introducing appropriate constraints according to previous work carried out on P6DMLT.[9] The potential energy surface was calculated

using a grid of 30°. Standard bond distances and angles were used and the remainder conformational angles were held fixed at their equilibrium values.

Molecular models of crystal structures were generated by using the CERIUS[2] software package[18] running on an Indigo 4000 Silicon Graphics workstation. Low-energy conformations previously derived from AM1 energy calculations[9] were used to build the crystal lattice with a geometry compatible with the crystal symmetry and parameters determined by diffraction experiments. X-ray and electron diffraction patterns of powders, fibers, and single crystals were calculated on-line from models and compared with the respective observed diagrams taking into account both spacings and intensities.

Packing energies of the crystal structures were estimated by force-field calculations using the AMBER program.[19,20] For calculations, the partial atomic charges, q_i and q_j, were parametrized for all atoms by fitting the AM1 molecular electrostatic potential to a set of atomic centered charges.[21,22] van der Waals and hydrogen-bond parameters were taken from the AMBER force-field libraries.[19,20] Hydrogen attached to nitrogen atoms were taken into account separately whereas a "united-atom" parametrization was applied to the aliphatic groups, *i.e.* the hydrogens attached to carbon atoms were not explicitly considered. A cut-off of 13.5 Å has been applied to all interactions.

Results and Discussion

A preliminary powder X-ray analysis of the P6DM(D,L)T series revealed that all these stereocopolyamides adopt a common type of crystal model which is not far from that adopted by the optically pure P6DMLT.[9,10] Furthermore, the diagrams produced by the copolyamide P6DM(D,L)T having a racemic composition were unique in showing a weak reflection at 4.9 Å. The same feature was observed for P6DM(D-L)T which is a polytartaramide with a D:L ratio equal to unity too but differing in the configurational sequence along the polymer chain. Such findings strongly suggested that definite structural modifications seem to take place in both polytartaramides as a consequence of the optical activity being fully compensated. In this work, fibers oriented by stretching and crystals grown from solution of the pure polymer P6DMLT and their optically compensated forms have been subjected to a detailed comparative analysis. Results obtained with these samples are in line with previous observations made on the whole copolyamide series and bring into light the structural relationship existing between the racemic copolyamide P6DM(D,L)T, the racemic mixture P6DM(D+L)T, and the optically pure polymer P6DMLT.

Crystal Sediments: DSC, X-ray, and ^{13}C CP−MAS NMR Analysis. The DSC thermograms obtained from crystal sediments of P6DMLT, the racemic copolymer P6DM(D,L)T, and the racemic mixture P6DM(D+L)T, both before and after annealing, are compared in Figure 1. The calorimetric data estimated by these means for the three systems under study are compared in Table 2. A double fusion peak reflecting a heterogeneous population of crystallites was observed in the first trace for the three cases. After annealing at temperatures intermediate between the two peaks, a single sharp endotherm corresponding to the higher melting peak present in the original traces was obtained in every case. For comparative purposes, the temperature associated with this single peak may be taken as the melting temperature of the polymer. Whereas P6DMLT and P6DM(D,L)T melt at 226 and 230 °C, respectively, a temperature of fusion near 250 °C was found for the racemic mixture. On the other hand, melting enthalpies of similar magnitude were registered for the three cases. The remarkable rise observed in melting temperature

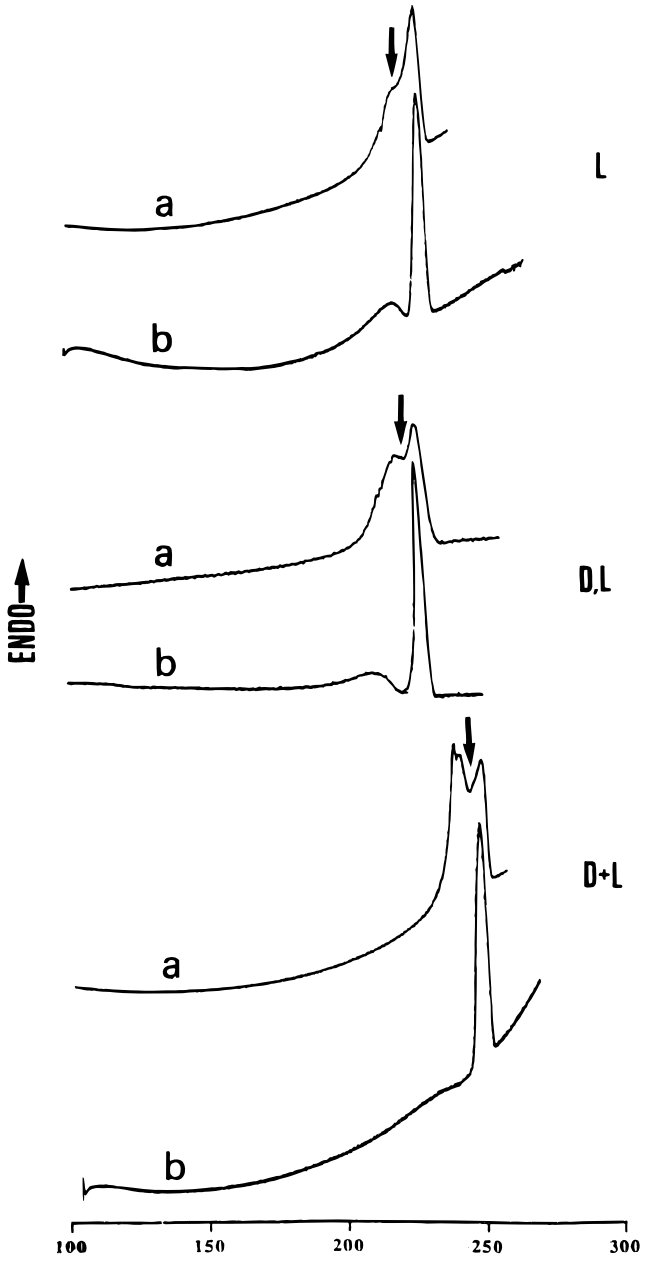

Figure 1. DSC traces of sediments of crystals grown in solution of polyamide P6DMLT, the racemic copolyamide P6DM(D,L)T, and the racemic mixture P6DM(D+L)T, before (a) and after (b) annealing for a few minutes at the indicated temperatures.

for P6DM(D+L)T strongly suggests the formation of a new crystal structure different from that of the corresponding polyenantiomers. A similar behavior has been described for racemate blends of poly(D-lactide) and poly(L-lactide) which is attributed to the existence of a stereocomplex, the existence of which is well documented.[23] Certain disubstituted poly(β-hydroxyalkanoate)s[24] display a similar behavior that has been interpreted in the same way. As we will see immediately below, the occurrence of a stereocomplex crystal made of a racemic lattice in which P6DMDT and P6DMLT are packed side-by-side in the ratio 1:1 is demonstrated in this work. The possibility that this system may be also stereoselectively associated either in solution or in the melt state is highly presumable in light of antecedents on crystalline stereocomplexes. However, no specific efforts have been made to evidence such a fact to date.

Table 2. Thermal Data of Polyamides:[a] Optically Pure Polymer, Racemic Polymer, and Racemic Mixture

		before annealing[b]			after annealing[b]		
polyamide	T_g (°C)	T_m (°C)	ΔH (cal g^{-1})	ΔS (cal mol^{-1} K^{-1})	T_m (°C)	ΔH (cal g^{-1})	ΔS (cal mol^{-1} K^{-1})
P6DMLT	106	230	14.8	7.6	232	13.5	7.0
P6DM(D,L)T	68	223	12.8	6.7	226	12.0	6.2
P6DM(D+L)T	96	244	11.3	5.6	250	9.0	4.4

[a] Sediments of crystals grown in glycerol. [b] Annealing between 200 and 210 °C for a period of 2 h.

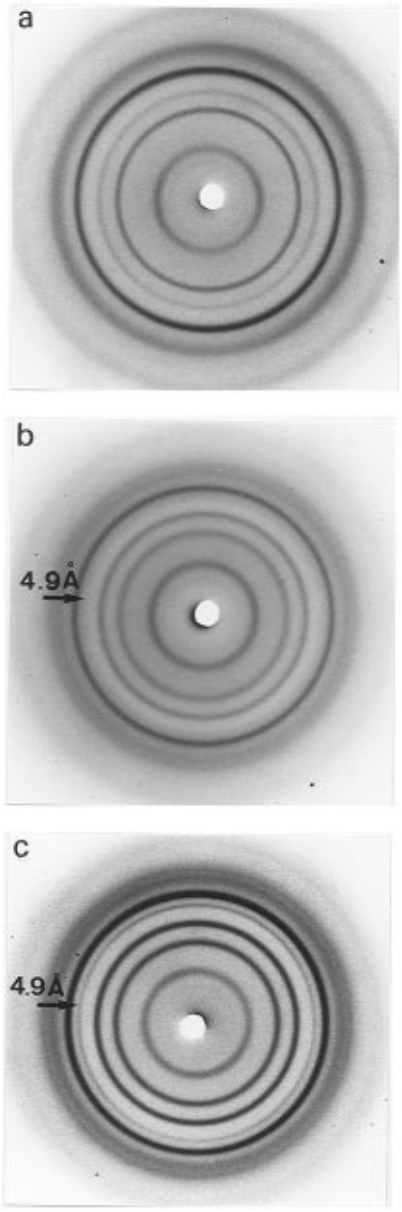

Figure 2. Debye−Scherrer X-ray diffraction patterns of crystal sediments of polyamide P6DMLT (a), the racemic copolyamide P6DM(D,L)T (b), and the racemic mixture P6DM(D+L)T (c). The 100 reflection spacing (4.95 Å) is clearly seen in (c), weak and diffuse in (b), and absent in (a).

When the crystal sediments were subjected to X-ray diffraction, the Debye−Sherrer diagrams shown in Figure 2 were obtained and the spacings observed for each case are compared in Table 3. Although they all show a great resemblance in both spacings and intensities, the pattern produced by the optically pure polymer is distinctly distinguished from the other two in that the characteristic medium-to-weak reflection appearing at 4.9 Å in optically compensated systems is there absent. The presence of such reflection should be associated therefore with the existence in the lattice of equal amounts of D- and L-tartaric units, whether they are contained in the same chain or are forming part of enantiomorphic optically pure chains.

CP−MAS ^{13}C NMR spectroscopy observations were in agreement with the conclusions drawn from the powder X-ray analysis. The spectra registered from crystal sediments of P6DMLT, P6DM(D,L)T, and P6DM(D+L)T are shown in Figure 3, where the spectrum obtained from P6DMLT in chloroform solution has been also included for comparison. The chemical shifts observed in each case together with their corresponding assignments are listed in Table 4. As can be seen, the carbonyl signal in the solid state spectra appears displaced about 1 ppm toward lower field with respect to its position in the solution spectrum. This displacement should be related to the unshielding effect caused by the intermolecular hydrogen bonding taking place in the crystal. Furthermore, the whole methylene region in the three solid state spectra appears displaced downfield relative to the spectrum obtained in solution. This is the effect that should be expected for the sample crystallized with the polymethylene sequence arranged in an *all-trans* conformation.

More relevant is the fact that the chemical shifts of the signals arising from the methylene carbons in the two racemic systems are nearly coincident and that they appear displaced upfield about 2 ppm when compared to the value observed for the optically pure polymer. As will be discussed below, X-ray diffraction and energy calculations results show that the conformation adopted by the polytartaramide chain is the same in the three cases. Therefore, the differences observed among them in the chemical shifts should be explained in terms of differences in the mode of packing of the chains in the crystal. Effects of this kind are known to operate in *n*-alkanes, where differences in displacements about 2 ppm were observed for polymorphs having in common the same *all-trans* conformation but differing in the symmetry of the lattice.[25] Moreover, since substantially the same chemical shifts are found for the racemic polymer and the racemic mixture, the crystal structure should be thought to be very similar in both cases. This structure will differ from that adopted by the optically pure P6DMLT in the manner in which the polymer chains are positioned in the lattice.

X-ray Diffraction of Fibers. The X-ray analysis of fibers has afforded definite evidence to establish the crystal structure of the racemic systems in relation to the structure earlier described for the homopolyamide P6DMLT.[9] The X-ray diagram registered from a fiber of P6DM(D,L)T, which was spun from the melt, is shown in Figure 4a. The pattern turns out to be practically indistinguishable from that arising from a fiber of P6DMLT obtained under similar conditions, except in the weak diffuse arced spot that appears on the equator with a spacing of 4.9 Å. This reflection obviously corresponds to the 4.9 Å ring observed in the powder diagram. The whole fiber pattern may be satisfactorily indexed on the basis of a monoclinic lattice of parameters $a = 4.95$ Å, $b = 13.70$ Å, $c = 13.20$ Å, $\alpha = 55°$, and

Table 3. Observed and Calculated Spacings (Å) for the Crystal Structure of the Racemic Stereocopolyamide P6DM(D,L)T and the Racemic Mixture P6DM(D+L)T

observed[a]										
fiber		single crystal[b]		sediment		calculated[c]				
D,L	D+L	D,L	D+L	D,L	D+L	D,L	D+L	*h*	*k*	*l*
5.63 s	5.70 s	5.59 s	5.80 s	5.54 s	5.74 s	5.62	5.83	0	2	0
4.92 vw	4.95 vw	4.92 vw	5.00 m	4.87 vw	4.91 m	4.92	4.95	1	0	0
4.51 vs	4.55 vs	4.50 vs	4.60 vs	4.50 vs	4.52 vs	4.51	4.56	1	1	0
2.50 m	2.50 m	2.46 m	2.46 w	2.50 m	2.50 m	2.46	2.50	2	0	0
10.86 vs	10.80 vs			10.83 vs	10.80 vs	10.81	10.90	0	0	1
6.86 s	6.80 s			6.85 s	6.80 s	6.83	6.88	0	2	1
4.11 s	4.10 s			4.11 s	4.15 s	4.10	4.18	0	−2	1
3.86 s	3.91 s			3.86 s		3.88	3.93	1	1	−1
6.03 vw						5.96	5.82	0	2	2
3.91 s					3.93 w	3.95	3.93	1	1	2
3.37 w						3.35	3.32	1	3	2
4.35 w						4.39	4.28	0	2	3
3.17 s					3.21 w	3.21	3.19	1	1	3
3.22 w	3.22 w					3.28	3.22	0	2	4
2.98 w	2.95 w					2.99	2.91	0	4	4
2.68 w										
2.54 vw	2.60 vw					2.57	2.55	0	2	5

[a] Visually estimated intensities denoted as vs = very strong, s = strong, m = medium, w = weak, vw = very weak. [b] Only basic spacings listed. [c] Calculated on the basis of monoclinic unit cells of parameters $\alpha = 4.95$ Å, $b = 13.70$ Å, $c = 13.20$ Å, $\alpha = 55°$, and $\beta = \gamma = 90°$, and $a = 4.95$ Å, $b = 13.70$ Å, $c = 12.93$ Å, $\alpha = 58°$, and $\beta = \gamma = 90°$ for P6DM(D,L)T and P6DM(D+L)T, respectively.

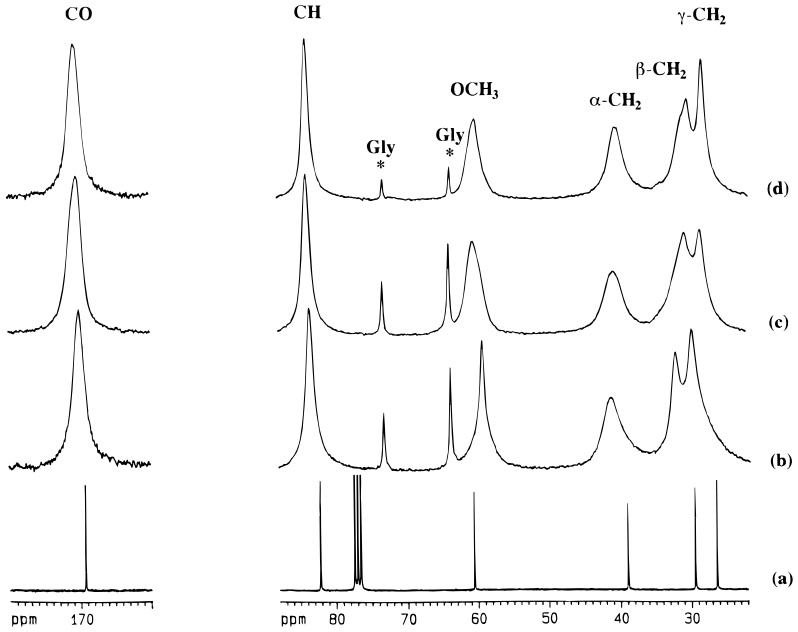

Figure 3. ^{13}C NMR (75.48 MHz) spectra of polyamides: (a) P6DMLT in chloroform solution, (b, c, and d) CP-MAS spectra of crystal sediments of P6DMLT, P6DM(D,L)T, and P6DM(D+L)T, respectively. The peaks labeled as Gly arise from residual glycerol.

Table 4. ^{13}C NMR Chemical Shifts of Polyamides in the Solid State[a]

	chemical shift (ppm)					
polyamide	CO	CH	OCH_3	α-CH_2	β-CH_2	γ-CH_2
P6DMLT	170.0	83.6	59.4	41.4	32.4	30.1
P6DM(D,L)T	170.4	83.9	60.5	40.8	30.6	28.4
PtDM(D+L)T	170.7	83.9	60.2	40.6	30.5	28.4
P6DMLT[b]	169.3	82.2	60.6	39.0	29.4	26.3

[a] Referenced to adamantane (29.5 ppm). [b] In chloroform solution referenced to TMS.

$\beta = \gamma = 90°$, containing two chains per unit cell (Table 3). The calculated density for this structure is 1.16 g mL^{-1}, in excellent concordance with the experimental value of 1.14 g mL^{-1}.

Fibers of P6DM(D+L)T obtained by stretching from the melt produced X-ray diagrams with much poorer orientation than those obtained with the racemic copolymer P6DM(D,L)T, and what is of most importance in this concern, they did not show signs of the 4.9 Å spacing. A similar result was obtained when fibers were prepared by pulling out from a solution in chloroform. On the contrary, diffraction patterns displaying similar orientation and scattering definition were obtained from both systems when fibers were prepared by stretching a concentrate solution of the polymer in formic acid; although the orientation achieved by this procedure is not high, the sharpness of the pattern enables clear resolution of the characteristic 4.9 Å reflection, which appears with comparable intensity in both cases (Figure 4b,c). The diffraction data collected for P6DM(D+L)T are consistent with a monoclinic structure comprised of an equimolar mixture of the two enantiomorphic polymers very similar to that described above for the racemic copolymer. The crystal parameters determined for this structure $a = 4.95$ Å, $b = 13.70$ Å, $c = 12.93$ Å, $\alpha = 58°$, and $\beta = \gamma = 90°$. The observed and calculated densities in this case are 1.14 and 1.15 g mL^{-1},

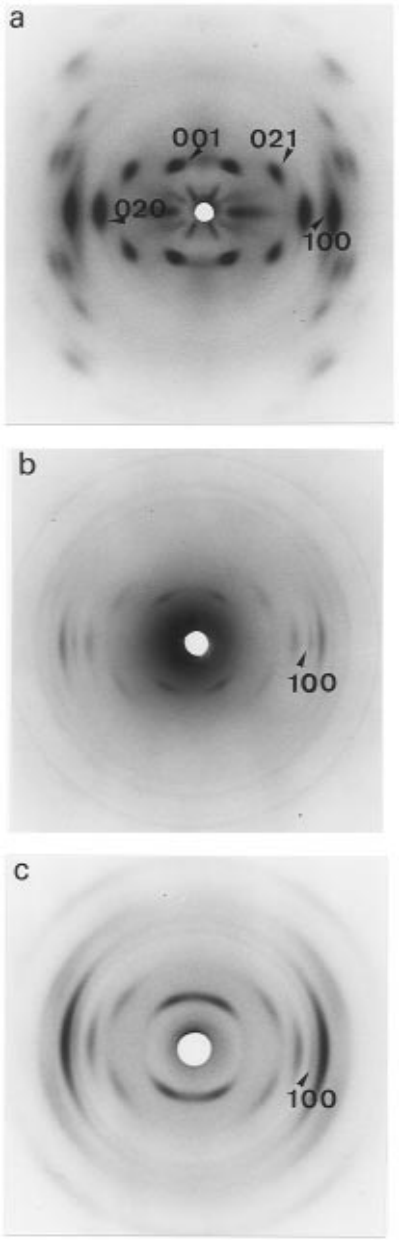

Figure 4. Fiber X-ray diagrams of copolyamide P6DM(D,L)T (a and b) and of the racemic mixture P6DM(D+L)T (c). In (a), the fiber was prepared by spinning from the melt. In (b) and (c), fibers were obtained by stretching from concentrated formic acid solutions. The fiber axis is vertical in the three cases.

respectively. Observed and calculated spacings are listed in Table 3, where correspondences with analogous data for the structures of P6DMLT and P6DM(D,L)T are brought into sight.

We may conclude from these results that poly(hexamethylene-2,3-di-*O*-tartaramide)s containing equal amounts of D- and L-tartaric units adopt the same type of crystal structure regardless the microstructure of the chain. The fact that this structure is not adopted in P6DM(D+L)T fibers that were stretched from the melt or pulled out from solutions in volatile solvents suggests that crystallization of D- and L-chains into the same crystal lattice must be a time dependent phenomenon. On the other hand, it should be worthy to remark that the geometry of the lattice resulting for the racemic systems is very close to that of polyamide P6DMLT;[9] in this case, however, the symmetry of the lattice is described as triclinic because the unit cell contains only one chain.

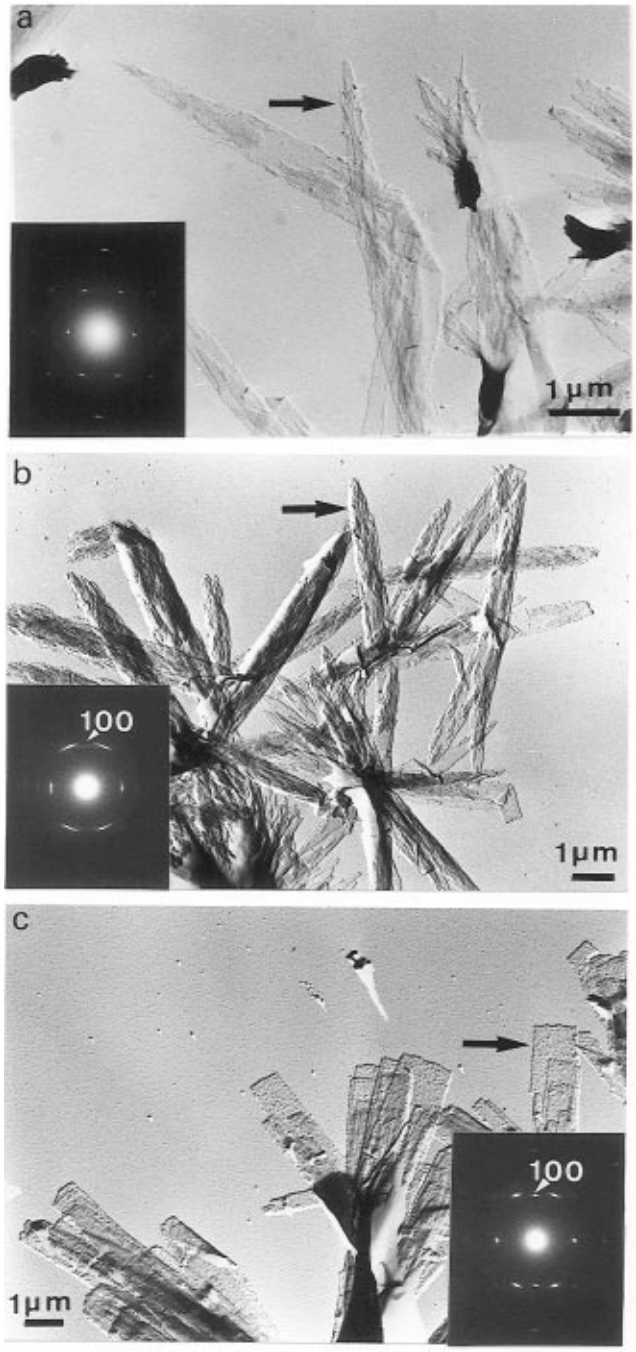

Figure 5. Lamellar crystals of polytartaramides crystallized in glycerol and their corresponding electron diffraction diagrams: (a) P6DMLT, (b) P6DM(D,L)T, and (c) P6DM(D+L)T.

Electron Microscopy. Further proof in support of the structural resemblance existing between copolyamide P6DM(D,L)T and the racemic mixture P6DM(D+L)T and the differences of these two compensated systems with homopolyamide P6DMLT was obtained from crystallization experiments carried out in solution. The crystals obtained from diluted solutions of polytartaramides in glycerol are shown in Figure 5, and a summary of the crystallization conditions and crystal characteristics is given in Table 5. Although crystallizations were carried out at different temperatures, the morphological features of the crystals and their diffracting properties are readily comparable. All of them consist of elongated lamellae having a width of about 1 μm and a thickness of 60−65 Å. The electron diffraction patterns recorded from such crystals are shown in the corresponding insets. The spacings and

Table 5. Crystallization Data and Crystal Characteristics of Polyamides

					crystal dimensions	
polyamide	solvent	T_d[a] (°C)	T_c[b] (°C)	t (h)	width (μm)	thickness (Å)
P6DMLT	glycerol	160	123	3	0.6	60
P6DM(D,L)T	glycerol	200	25	3	0.8	65
P6DM(D+L)T	glycerol	205	150	3	0.6	60
P6DM(D-L)T	MPD[c]	190	80	2.5	≤0.2	60

[a] Disolution temperature. [b] Crystallization temperature. [c] 2-Methyl-2,4-pentanediol.

positions of the reflections appearing in the respective patterns are consistent with the geometry of the crystal lattice proposed for each case. Nevertheless, a comparative inspection of the diagrams revealed details of significance for the interpretation of the structure. The characteristic 4.9 Å reflection discussed above and indexed as 100 is clearly perceived in the diagram arising from crystals of P6DM(D+L)T whereas it is absent in the diagram of P6DMLT. Such reflection is present also in the diffraction pattern of copolyamide P6DM(D,L)T but now as a weak streak for which the intensity slightly varies from crystal to crystal. As we will see below, the appearance of the 4.9 Å reflection is associated with the change in symmetry of the lattice resulting from doubling the number of chains contained in the unit cell; a glide plane parallel to *b* relating the two enantiomeric units in the lattice may account for the systematic 0*kl* extinctions observed for odd values of *k* in the diagrams of the optically compensated systems. Incidentally, 0*k*l reflections are observed in the pattern of P6DMLT instead of 0*k*0, indicating that the *c* axis of the crystal is tilted about 30° with respect to the electron beam. This means that the 001 plane of the crystal must be lying parallel to the basal plane of the lamella.

At this point it is advisable to be reminded that the interpretation of P6DM(D,L)T as consisting of a random distribution of D- and L-configurations is not supported by any direct evidence.[10] Since no signs of ordered microstructures were found, the compounds were assumed to be statistical stereocopolymers according to what could be reasonably expected from the method used for their preparation. For that reason, the racemic copolyamide P6DM(D−L)T was synthesized from a D−L-diacid sesquiomer in order to ensure the coexistence of D- and L-units within the same chain arranged in an uneven distribution. In this polyamide, no more than two successive tartaric units with the same configuration can occur.[10] Crystallization from solution of this polyamide led to sheaves composed of thin long crystals as those shown in Figure 6. The electron diffraction pattern arising from one of these bundles is concordant with that obtained from lamellar crystals of copolyamide P6DM(D,L)T, except in the additional reflection indexed as 021. The existence of such reflection is quite reasonable if one considers that the orientation of the crystals around the bundle axis must be random. What is really outstanding in these patterns is that the 100 reflection becomes observed with the same characteristics as in the patterns yielded by copolyamide P6DM(D,L)T. Moreover, the powder X-ray diagram recorded from a sediment of crystals of P6DM(D-L)T (now shown) turns to be indistinguishable also from that obtained from P6DM(D,L)T. Such coincidences not only validate the interpretation of the 4.9 Å reflection arising as a result of the coexistence of D- and L-units in the same crystal

Figure 6. Sheaves of polyamide P6DM(D−L)T grown in 2-methyl-2,4-pentanediol at 80 °C. Inset: Electron diffraction from the indicated structure.

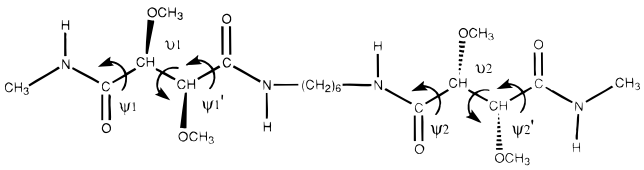

Figure 7. Chemical formula of model compound of the alternating copolyamide P6DM(D,L)T (1:1) with indication of the dihedral angle notation used in this work.

but provide also further evidence in favor of the random structure assumed for the copolyamide P6DM(D,L)T.

Conformational Analysis of the Copolytartaramide P6DM(D,L)T. Previous AM1 calculations carried out on P6DMLT showed that the arrangement preferred by this polymer entails the tartaric acid moiety in a *gauche* conformation and the amide group rotated out of the plane of the zigzag polymethylene segment. As a consequence, the resulting chain is compressed in about 2 Å per repeating unit, in agreement with the axial repeat estimated by X-ray diffraction. Fiber X-ray diffraction data from both P6DM(D,L)T and P6DM(D+L)T have shown that the chain is contracted in a similar extent in these cases.

In order to evaluate the effect that the configuration of the tartaric unit may exert on the conformation of the polytartaramide chain, the model molecule represented in Figure 7 was analyzed by AM1 calculations. In this molecule the two tartaric units are in opposite configurations, as corresponds to an alternating P6DM(D,L)T stereocopolymer. A conformational map was computed under the following constraints: $\Psi_1 = \Psi_2 = -\Psi_1' = -\Psi_2'$ and $\upsilon_1 = \upsilon_2$. Those cases implying the condition $\Psi = \Psi'$ were discarded since previous calculations made on P6DMLT revealed that they were incompatible with experimental data.[9] The resulting steric map drawn with the contour lines at increments of 1 kcal mol^{-1} is depicted in Figure 8. Two equivalent low-energy conformation regions corresponding to those found for optically pure P6DMDT and P6DMLT with respective dihedral values of $\Psi = -\Psi' \approx 60°$, $\upsilon \approx 180°$ and $\Psi = -\Psi' \approx -60°$, $\upsilon \approx 180°$ were found for P6DM(D,L)T. The two regions are indistinguishable due to the racemic composition of the model molecule. The polymer chain built with dihedrals within any of the two regions will be in the absolutely favored conformation. Similar conclusions would be drawn if the configurations were distributed at random following Bernouillian statistics, which is actually the case for the

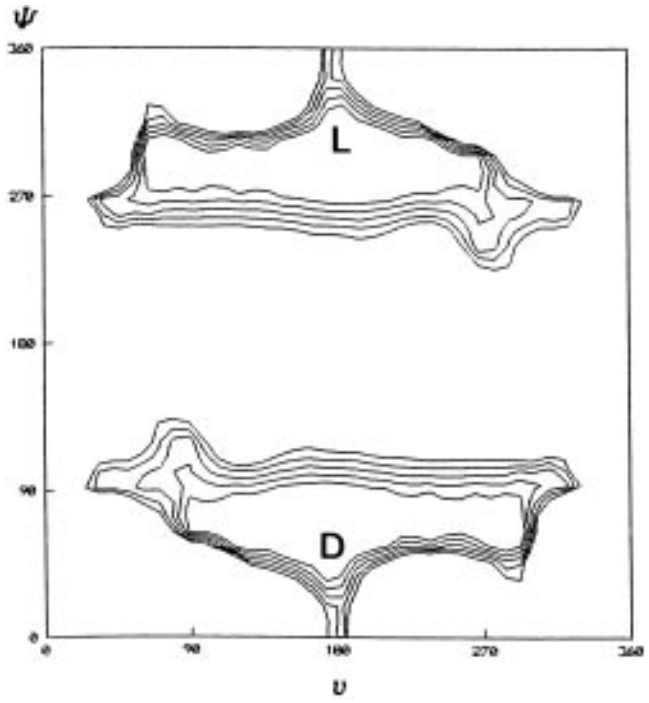

Figure 8. Conformational map of the model compound represented in Figure 7.

copolyamides under study. The present results allow us to assume the same conformation for both homopolyamides and D,L-copolyamides, in agreement with fiber X-ray diffraction data.

Crystal Modeling and Diffraction Pattern Simulation. We have made use of the CERIUS[2] software package to model and refine the crystal structure of P6DM(D,L)T and P6DM(D+L)T. This program enables one to observe on-line the changes in the X-ray and electron diffraction simulated patterns as the molecular model is adjusted. Such methodology has proven to be useful in the structural study of polymers for which abundant diffraction data are available provided that the conformation of the chain in the gas-phase state is known.[26,27] Furthermore, we have recently used this program in the analysis of the crystal structure of P6DMLT in combination with the linked-atom least-squares methodology.[9] Results obtained from both methods were in good agreement, which may be taken as proof of the reliability of CERIUS in the analysis of these types of systems.

Lattice parameters estimated from experimental diffraction data were used for building the crystal. The volume of the unit cell and the experimental density were used to determine the number of chains per unit cell, two in both cases. This together with symmetry considerations based on diffraction extinctions led us to assume a monoclinic space group *P*1*b*1 as a reasonable crystal model for both P6DM(D,L)T and P6DM(D+L)T. In this structure the two chains contained in the unit cell are related by a glide plane parallel to the *b* axis of the crystal; $k = 2n$ is the condition limiting possible 0*kl* reflections, whereas no conditions apply to *hkl* reflections with *h* different from 0. This is in full agreement with both X-ray and electron diffraction observations.

Firstly the crystal structure of P6DM(D+L)T was built. For this the asymmetric unit arranged in the conformation described previously for P6DMLT was placed at the origin of the unit cell and the lattice generated by application of the *P*1*b*1 space group

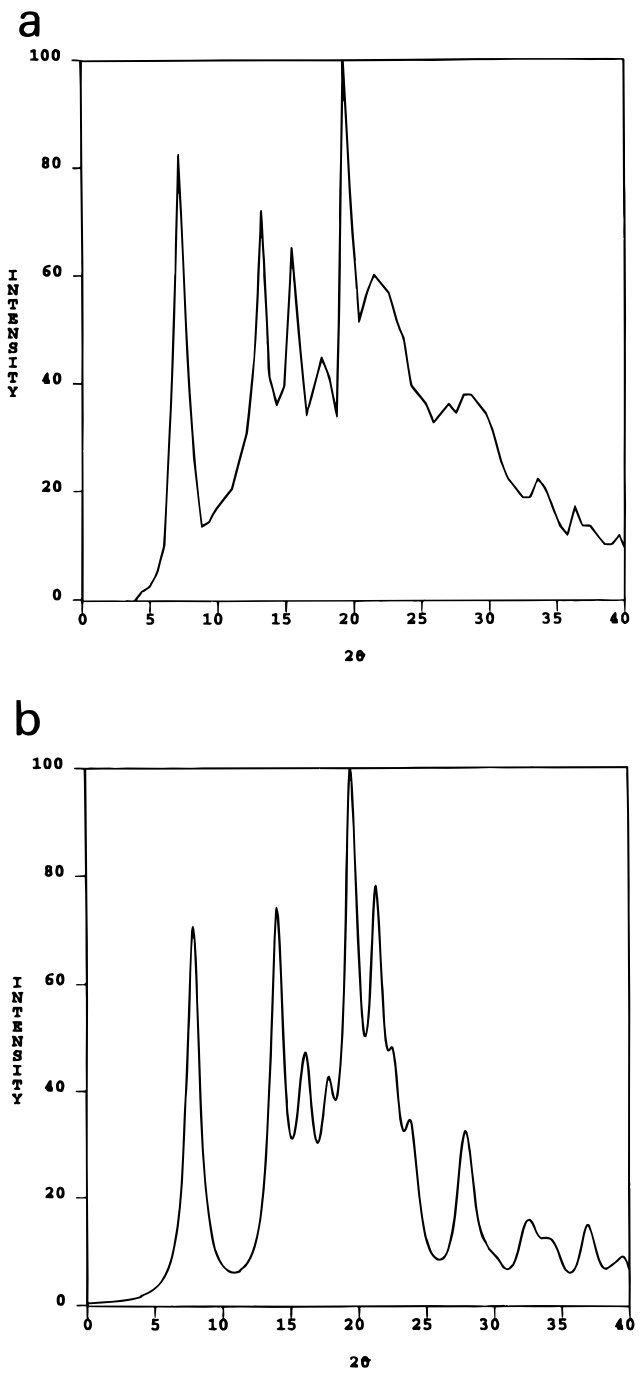

Figure 9. Observed (a) and calculated (b) powder X-ray patterns of the racemic mixture P6DM(D+L)T.

symmetry. The orientation of the chain with respect to the geometry of the lattice is primarily decided by hydrogen-bonding requirements. By analogy with the crystal structure described for P6DMLT, hydrogen bonds were set along the *a* direction of the crystal, which corresponds to the preferential direction of crystal growing. Then the position of the chain was adjusted to obtain a good agreement between experimental and calculated X-ray powder diffraction profiles (Figure 9). The resulting structure was further readjusted until good agreement was obtained between calculated and observed intensities for both X-ray fiber and single crystal electron diffraction patterns. Numerical values of the observed and calculated intensities for the seven rings present in the powder X-ray diagram for the three systems under study are compared in Table 6. Particular attention was devoted to reproduce the 4.9 Å

Table 6. Comparison between Observed[a] and Calculated[b] Intensities for the X-ray Powder Diagrams of Polyamides

		P6DMLT			P6DM(D+L)T			P6DM(D,L)T		
ring	d_{hkl}[c]	hkl[d]	I_o	I_c	hkl[e]	I_o	I_c	hkl[e]	I_o	I_c
1	11.3−10.8	0 0 1	53	63	0 0 1	97	93	0 0 1	86	88
2	6.8−6.3	0 1 1	68	62	0 2 1	88	91	0 2 1	82	89
3	5.7−5.4	0 1 0	19	20	0 2 0	34	31	0 2 0	41	37
4	4.9	−	−	−	1 0 0	42	33	1 0 0	9	16
5	4.6−4.5	1 0 0	100	114	1 1 0	82	100	1 1 0	91	96
		1 0 1			1 1 1			1 1 1		
6	4.2−4.1	0 −1 1	92	101	0 −2 1	100	91	0 −2 1	10	110
		1 0 2			1 1 2			1 1 2	0	
7	2.5	−2 1 0	7	9	2 0 0	9	14	2 0 0	10	6

[a] Measured by densitometry. [b] Calculated by CERIUS for the corresponding simulated models. [c] Observed spacing ranges. [d] Indexes for a triclinic unit cell of parameters $a = 5.00$, $b = 6.84$, $c = 13.20$, $\alpha = 61.5°$, $\beta = 90.0°$, and $\gamma = 111.6°$. [e] Indexes for the monoclinic unit cells respectively defined for the racemic polymer and the racemic mixture (see Table 7).

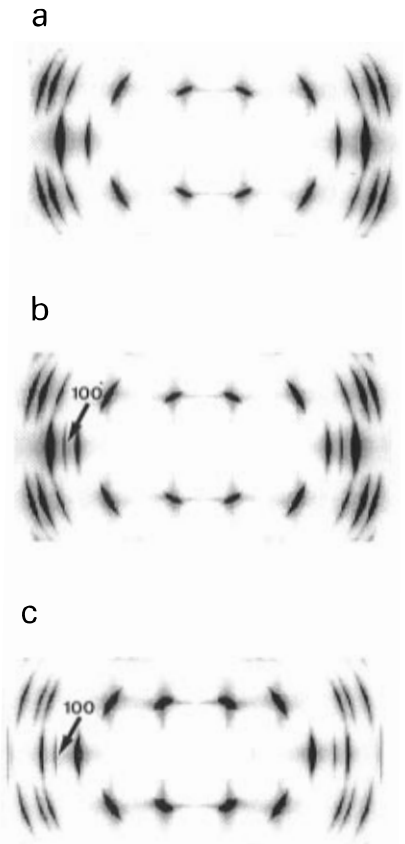

Figure 10. Simulated fiber X-ray diffraction patterns of the racemic mixture P6DM(D+L)T (b) and the racemic copolyamide P6DM(D,L)T (c). The corresponding region of the simulated diagram for the optically pure polyamide P6DMLT is reproduced in (a) for comparison.

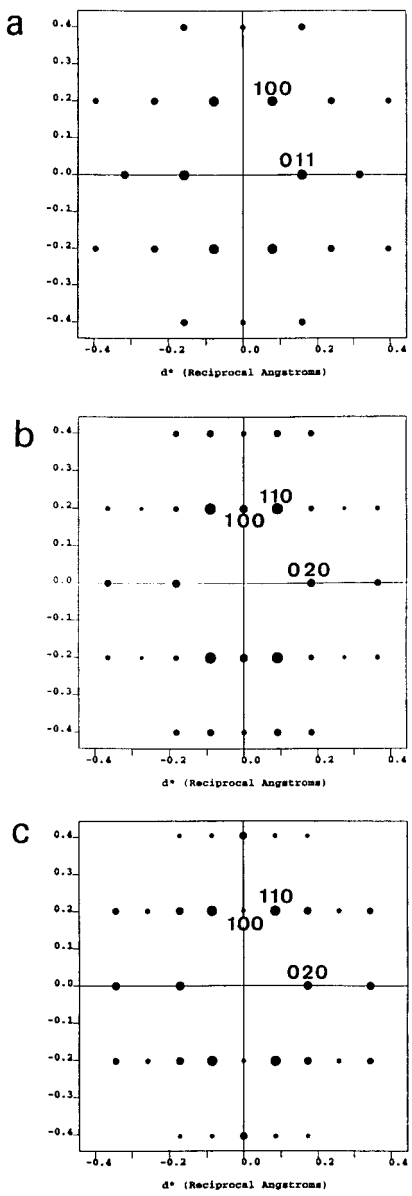

Figure 11. Simulated single crystal diffraction pattern of the racemic mixture P6DM(D+L)T (b) and the racemic polymer P6DM(D,L)T (c). The simulated diagram for polyamide P6DMLT is reproduced in (a) for comparison. Note the different intensity displayed by the 100 reflection in each case, in agreement with experimental observations.

reflection, the intensity of which appeared to be highly sensitive to variations in the relative orientation of the two enantiomeric chains. The final simulated fiber and single crystal diffraction patterns are shown in Figures 10b and 11b, illustrating the satisfactory concordance attained with the experimentally observed ones. A projection down the *c* axis of the resulting lattice is shown in Figure 12b. The structure may be envisaged as deriving from the crystal structure of P6DMLT by replacing one of out two L-chains by the D-enantiomorph; the relative orientation of the two enantiomeric chains in the lattice is defined by the glide plane.

The same strategy was followed in the analysis of the racemic copolyamide P6DM(D,L)T. The crystal lattice made of random copolyamide chains could be formally represented by a unit cell in which each asymmetric unit is composed of one L- and one D-unit, both placed in the same position within half of the cell. Due to the difficulty in modeling a chain with a statistical distribution of D- and L-units, we used an asymmetric unit comprised of two chemical repeating units in opposite configuration. As a consequence, the axial repeat is doubled and the unit cell contains four chemical repeat-

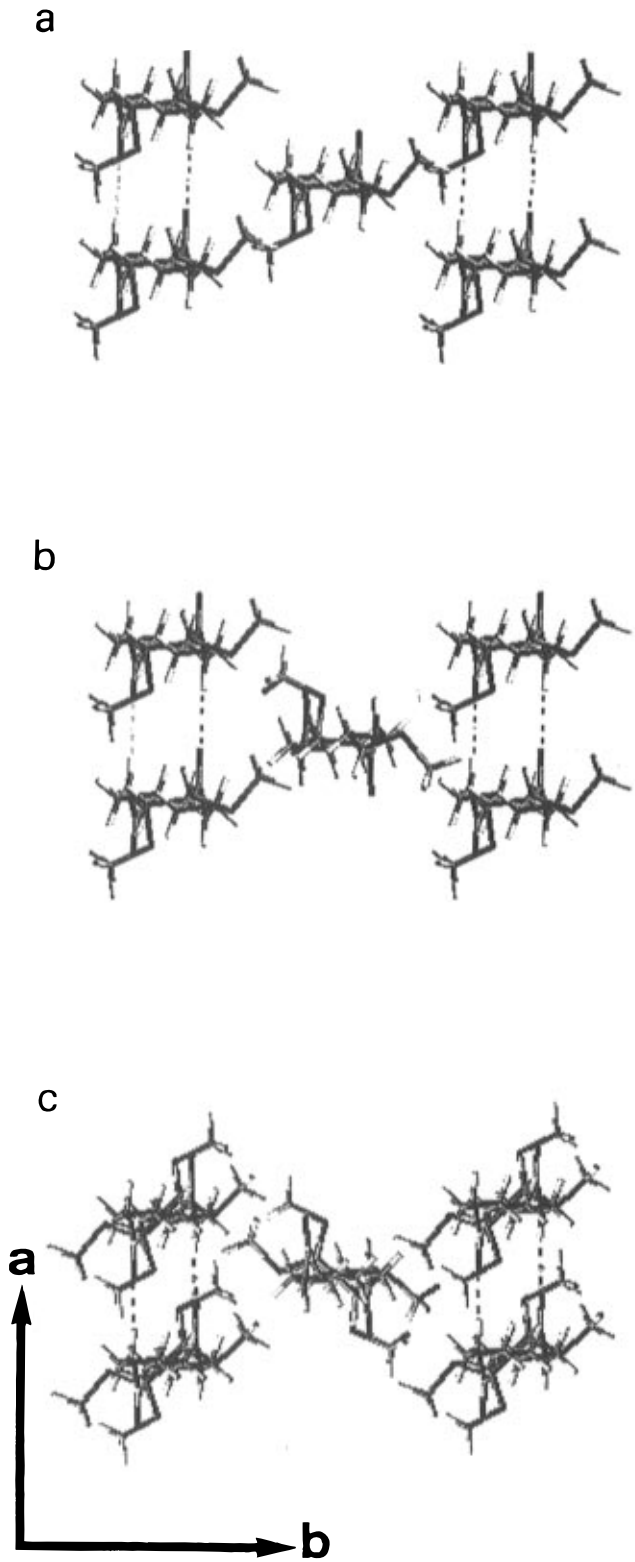

Figure 12. Projection down the *c* axis of the simulated crystal structure for P6DMLT (a), P6DM(D+L)T (b), and P6DM(D,L)T (c). In order to make comparison straightforwardly, two chains have been used for representation in (a) although the unit cell of this structure is primitive (see the text and Table 7).

ing units. Even though an alternating copolymer is actually being represented, the effects of the stereochemical constitution on packing and diffraction are considered to be adequately mimicked for comparative purposes. The relative orientation of the chains in the lattice was chosen such that the symmetry requirements of the space group *P*1*b*1 were satisfied. The correlation attained between observed and calculated intensities for the powder diagrams is of a quality similar to that achieved in the case of the P6DM(D+L) structure (Table 6). The projection of the idealized structure down the *c* axis is depicted in Figure 12c, where analogies with similar representations of polyamides P6DMLT and P6DM(D+L)T are brought into evidence. The fiber and single crystal diffraction diagrams calculated for this structure compare well with observed data; in particular, the 4.9 Å reflection could be satisfactorily reproduced with the adequate intensity (Figures 10c and 11c).

A comparison of the main features displayed by the crystal structures of the three systems concerned in this work is given in Table 7. Since the conformation of the chain is the same for the three cases, differences in the crystal structure arise solely from differences in the spatial orientation of the tartaric units within the lattice. A similar scheme of hydrogen bonds with substantially the same N···O distances and N−H−O angles is adopted by the three structures. It should be remarked that a unit cell containing two chains has been used here for describing the structure of P6DMLT, although the formal one is primitive.[9] By this means the orthogonal geometry of the lattice in the *C* plane becomes apparent, and comparison with the crystal structure of the racemic forms may be done more straightforwardly.

Crystal Packing Energy Calculations. In order to ascertain the influence of the configuration on the relative stability of the crystal, comparative force-field calculations were carried out on the three systems under study. Computations were performed on an infinite crystal which was built by applying periodic boundary conditions to the respective unit cells in the corresponding space groups. Results are included in Table 7, where the relative energies are expressed in kcal/mol of residue. As can be seen, the interactions of the chains in the unit cell of both P6DM(D+L)T and PDM(D,L)T are unfavored by less than 1 kcal/mol of residue with respect to those operating in the homopolymer. In order to check the compatibility of these results with hydrogen-bond formation, the central molecule in the models displayed in Figure 12 was rotated around the chain axis by an angle θ and the intermolecular energy computed at intervals of 2°. In the case of the optically compensated systems, the second chain in the unit cell is rotated by an opposite angle in order to preserve the symmetry of the crystal. The whole examined range was restricted to ±8° since out of this range hydrogen bonds cannot be set. The resulting potential energies are compared in Figure 13. In the all three cases the molecular orientation with minimum energy corresponds to that found by CERIUS, which had been established on the exclusive basis of simulation criteria. As expected, the arrangement corresponds to that enabling an optimum geometry of hydrogen bonds.

Concluding Remarks

The above study combines X-ray, electron microscopy, and ^{13}C CP−MAS NMR measurements with computational methods to investigate the crystal structure of racemic poly(hexamethylene-di-*O*-methyl-D,L-tartaramide) [(P6DM(D,L)T] and the equimolar mixture of poly(hexamethylene-di-*O*-methyl-D- and -L-tartaramide)s [P6DM(D+L)T] with reference to the structure previously described by us for the optically pure polymer P6DMLT.[9] The three systems are shown to be highly crystalline; the melting point of the racemic mixture is 250 °C, considerably higher than 232 °C, the melting

Table 7. Compared Structural Data for Polyamide P6DMLT, the Racemic Copolyamide P6DM(D,L)T, and the Racemic Mixture P6DM(D+L)T

		density (g mL^{-1})			hydrogen bonds		
polyamide	a_0, b_0, c_0 (Å) α, β, γ (deg)	obsd	calcd	space group	N···O (Å)	N···H···O (deg)	ΔE^a
P6DMLT[b]	5.00, 12.65, 13.20 59, 90, 90	1.13	1.20	*P*1	2.90	170	0.0
P6DM(D,L)T	4.95, 13.75, 13.20 55, 90, 90	1.14	1.15	*P*1*b*1	2.93	169.7	0.7
P6DM(D+L)T	4.95, 13.75, 12.93 58, 90, 90	1.14	1.16	*P*1*b*1	2.89	170.6	0.3

[a] Energy in kcal/mol of residue. [b] Parameters for a unit cell containing two identical chains; the true unit cell is primitive with parameters: $a = 5.00$ Å, $b = 6.84$ Å, $c = 13.20$ Å, $\alpha = 61.5°$, $\beta = 90°$, and $\gamma = 111.6°$.

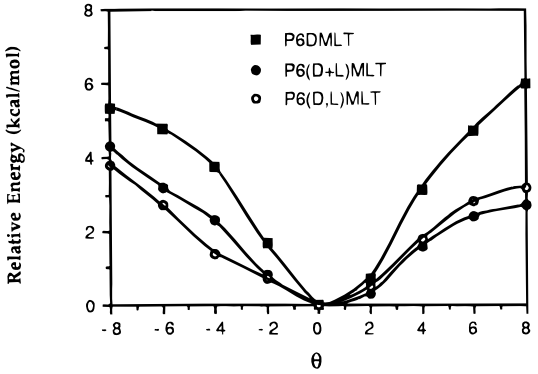

Figure 13. Potential energy surface obtained by rotation of the polymer chain around its axis (θ) for the optically active P6DMLT and the optically compensated systems P6DM(D,L)T and P6DM(D+L)T.

temperature of the diisotactic homopolymer, whereas the racemic polymer melts at 226 °C.

A comparative diffraction analysis has been performed on powders, fibers, and single crystals for the three systems under study. The different types of diagrams were coincident in showing that the geometry and parameters of the lattice are very similar for the three cases. The presence of an additional reflection in diagrams arising from either P6DM(D,L)T or P6DM(D+L)T, together with some slight variations in the relative intensity of the scattering profile, was the only feature distinguishing such systems from P6DMLT. Such differences are interpreted to be due to the higher crystal symmetry associated with the optically compensated systems. On the other hand, AM1 calculations carried out on a single chain have shown that the conformation preferred by the D,L-stereocopolytartaramide is the same as that preferred by the homopolymer. This arrangement has the tartaric acid moiety in a *gauche* conformation and the amide group rotated out of the plane of the polymethylene segment, which is in a fully extended *all-trans* conformation. NMR results are in agreement with the conclusions drawn from the conformational analysis and corroborate the structural differences between the optically pure polymer and the optically compensated systems evidenced earlier by diffraction experiments.

A triclinic unit cell in the space group *P*1 containing one chain was reported for P6DMLT.[9] This structure was taken as a safe guidance for interpreting the structural data of the optically compensated systems. Modeling simulation methods allowed us to build the crystal structure of both P6DM(D,L)T and P6DM(D+L)T as a monoclinic lattice in the space group *P*1*b*1 containing two chains which are related by a glide plane parallel to the *b* axis of the crystal. A close similarity exists between the optically active and inactive lattices which is clearly evidenced when the structure of P6DMLT is represented by a unit cell containing two identical chains (see Table 7 and Figure 12). In fact, the racemic *P*1*b*1 crystal may be generated from the optically active *P*1 crystal by systematic replacing one of out two chains by its enantiomorph. The racemic copolymer is assumed to adopt a similar lattice but with an identical statistical D,L-chain occupying the two positions of the unit cell. It should be remarked that the essentials of the structures, i.e. the scheme in which hydrogen bonds are arranged and the chain conformation, are common for both types of lattices. Energy calculations revealed that the crystal packings adopted by the three systems are of comparable stability.

Our results prove that the isomorphic replacement between D- and L-tartaric units in poly(hexamethylene-di-*O*-methyltartaramide)s is feasible without altering substantially the side-by-side packing of the chains. By this means the crystallinity of the polymer is largely retained and related properties may be convincingly explained. To our knowledge, this is the first time that a racemic crystal made of a nonpolypeptidic polyamide is described. The finding is considered to be of particular relevance because of the high density of stereocenters present in the polytartaramide chain and the repercussion that it may have on the design of crystalline polyamides from multichiral monomers.

Acknowledgment. Financial support for this work was given by CICYT, MAT-93-555-CO2. The authors are indebted to CESCA for computational facilities.

References and Notes

(1) Bou, J. J.; Iribarren, I.; Rodríguez-Galán, A.; Muñoz-Guerra, S. *Biodegradable Polymers and Plastics*; Vert, M., Ed.; Royal Society of Chemistry: Cambridge, UK, 1992; p 271.
(2) Bou, J. J.; Ruíz, P.; Iribarren, I.; Rodríguez-Galán, A.; Muñoz-Guerra, S. *Proceedings of the 11th European Conference on Biomaterials*; Pisa, 1994, p 406.
(3) Regaño, C.; Iribarren, I.; Vidal, X.; Martínez de Ilarduya, A.; Bou, J. J.; Muñoz-Guerra, S. *Proceedings of the 12th European Conference on Biomaterials*; Porto, 1995, p 81.
(4) Ruíz-Donaire, P.; Bou, J. J.; Muñoz-Guerra, S.; Rodríguez-Galán, A. *J. Appl. Polym. Sci.* **1995**, *58*, 41.
(5) Rodríguez-Galán, A.; Bou, J. J.; Muñoz-Guerra, S. *J. Polym. Sci., Polym. Chem. Ed.* **1992**, *30*, 713.
(6) Bou, J. J.; Rodríguez-Galán, A.; Muñoz-Guerra, S. *Macromolecules* **1993**, *26*, 5664.
(7) Bou, J. J.; Iribarren, I.; Muñoz-Guerra, S. *Macromolecules* **1994**, *27*, 5263.
(8) Bou, J. J.; Muñoz-Guerra, S. *Polymer* **1995**, *36*, 181.
(9) Iribarren, I.; Alemán, C.; Bou, J. J.; Muñoz-Guerra, S. *Macromolecules* **1996**, *29*, 4937.
(10) Regaño, C.; Martínez de Ilarduya, A.; Iribarren, I.; Rodríguez-Galán, A.; Galbis, J. A.; Muñoz-Guerra, S. *Macromolecules* **1996**, *29*, 8404 (preceding paper in this issue).
(11) Tadokoro, H. *Makromol. Chem.* **1981**, *4*, 129.
(12) Dumas, P.; Spassky, N.; Sigwalt, P. *Makromol. Chem.* **1972**, *156*, 55. Matsubayashi, H.; Chatani, Y.; Tadokoro, H.; Dumas, P.; Spassky, N.; Sigwalt, P. *Macromolecules* **1977**, *10*, 996.

(13) Tsuboi, M.; Wada, A.; Nagashima, N. *J. Mol. Biol.* **1961**, *3*, 705. Elliot, A.; Fraser, R. D. B.; MacRae, T. P. *J. Mol. Biol.* **1965**, *11*, 821. Sakahikara, H.; Takahashi, Y.; Tadokor, H.; Oguni, N.; Tani, H. *Macromolecules* **1973**, *6*, 205. Hatada, K.; Shimizu, S.; Terawaky, Y.; Ohta, K.; Yuki, H. *Polym. J.* **1981**, *13*, 811. Grenier, D.; Prud'homme, R. E. *J. Polym. Sci., Polym. Phys. Ed.* **1984**, *22*, 577. Voyer, R., Prud'homme, R. E. *Eur. Polym. J.* **1989**, *25*, 365. Ikada, Y.; Khosrow, J.; Tsusji, H.; Hyon, S-H. *Macromolecules* **1987**, *20*, 906. Okihara, T.; Tsuji, M.; Kawaguchi, A.; Katayama, K.; Tsuji, H.; Hyon, S.-H.; Ikada, Y. *J. Macromol. Sci., Phys.* **1991**, *B30*, 119.

(14) Lavallée, C.; Prud'homme, R. E. *Macromolecules* **1989**, *22*, 2438. Ritcey, A. M.; Prud'homme, R. E. *Macromolecules* **1992**, *25*, 972.

(15) Tsuji, H.; Horii, F.; Hyon, S-H., Ikada, H. *Macromolecules* **1991**, *24*, 2719.

(16) Thiem, J.; Bachmann, F. *Trends Polym. Sci.* **1994**, *12*, 425. Bachmann, F.; Thiem, J. *Makromol. Chem.* **1993**, *194*, 1035. Hashimoto, K.; Wibullucksanakul, S.; Matsuura, M.; Okada, M. *J. Polym. Sci., Polym. Chem. Ed.* **1993**, *31*, 3141. Kiely, D. E.; Chen, L.; Lin, T-H. *J. Am. Chem. Soc.* **1994**, *116*, 571. Bueno, M.; Galbis, J. A.; García-Martín, M. G.; De Paz, M. V.; Zamora, F.; Muñoz-Guerra, S. *J. Polym. Sci., Part A: Polym. Chem.* **1995**, *33*, 299.

(17) Dewar, M. J. S.; Zoebisch, E. G.; Healy, E. F.; Stewart, J. J. P. *J. Am. Chem. Soc.* **1985**, *107*, 3902.

(18) CERIUS^2 1.6, Molecular Simulations Inc., Burlington, Massachussets.

(19) Weiner, S. J.; Kollman, P. A.; Case, D. A.; Singh, U. C.; Ghio, C.; Alagona, G.; Weiner, P. J. *J. Am. Chem. Soc.* **1984**, *106*, 765.

(20) Weiner, S. J.; Kollman, P. A.; Nguyen, D. T.; Case, D. A. *J. Comput. Chem.* **1986**, *5*, 277.

(21) Alhambra, C.; Luque, F. J.; Orozco, M. *J. Comput. Chem.* **1994**, *15*, 12.

(22) Ferenczy, G. G.; Reynolds, C. A.; Richards, W. G. *J. Comput. Chem.* **1990**, *11*, 159.

(23) Tsuji, H.; Ikada, Y. *Macromolecules* **1992**, *25*, 5719; **1993**, *26*, 6918. Tsuji, H.; Hyon, S-H.; Ikada, Y. *Macromolecules* **1991**, *24*, 5651; **1991**, *24*, 5657; **1992**, *25*, 2940.

(24) Ritcey, A. M.; Brisson, J.; Prud'homme, R. E. *Macromolecules* **1992**, *25*, 2705.

(25) Vanderhart, D. L. *J. Magn. Res.* **1981**, *44*, 117.

(26) Voigt-Martin, I. G.; Garbella, R.; Schumacher, M. *Macromolecules* **1992**, *25*, 961.

(27) Voigt-Martin, I. G.; Simon, P.; Yan, D.; Yakimansky, A.; Bauer, S.; Ringsdorf, H. *Macromolecules* **1995**, *28*, 243.

MA960473J